ISSN 0965-545X, Polymer Science, Ser. A, 2008, Vol. 50, No. 2, pp. 181–189. © Pleiades Publishing, Ltd., 2008.
Original Russian Text © I.A. Chmutin, N.G. Ryvkina, E.A. Zubova, L.I. Manevich, 2008, published in Vysokomolekulyarnye Soedineniya, Ser. A, 2008, Vol. 50, No. 2, pp. 295–305.

Chain Diffusion in Semicrystalline Polyethylene: Dielectric Relaxation[1]

I. A. Chmutin[a], N. G. Ryvkina[a], E. A. Zubova[b], and L. I. Manevich[b]

[a] *Institute of Radio Engineering and Electronics, Russian Academy of Sciences (Fryazino Branch), pl. Vvedenskogo 1, Fryazino, Moscow oblast, 141190 Russia*
[b] *Semenov Institute of Chemical Physics, Russian Academy of Sciences, ul. Kosygina 4, Moscow, 119991 Russia*
e-mail: tchmutin@mail.ru

Received December 20, 2006;
Revised Manuscript Received May 29, 2007

Abstract—The experimental data on high-temperature dielectric relaxation α_c in linear PE samples with different thermal prehistories (slow cooling, quenching, and annealing) are described. The measurements are conducted at temperatures ranging from 0 to 80°C. Dielectric losses are measured with a high accuracy at frequencies varying from 10^{-2} to 10–10^6 Hz. These dielectric measurements allow one to reveal changes in the frequency dependence of losses with temperature. This effect of thermal prehistory of the sample and applied stress is explained within the framework of the molecular model of chain diffusion between crystalline and amorphous phases in PE.

DOI: 10.1134/S0965545X08020132

INTRODUCTION

In 1991, chain diffusion between crystalline and amorphous phases in PE has been confirmed by NMR measurements [1]. In 1998, direct NMR experiments demonstrated that chain flip motions in the PE crystallite by the lattice half-period are accompanied by chain reorientation with a rotation angle of 180° [2]. Therefore, after flip motions and reorientation, the chain is reincorporated into a crystalite. Similar processes of chain diffusion between phases have been observed only for several polymers (PE, PVDF, PTFE, POM, isotactic PP, and PEO). This process should manifest itself as a mechanical relaxation of the above polymers, and chain flips in the PE crystallites should be detected by dielectric methods for weakly oxidized samples.

Indeed, the occurrence of high-temperature relaxation α_c in solid PE has been revealed by using dielectric methods 50 years ago [3–6]. Unusual features of this process has triggered further intensive dielectric [7–11] and mechanical studies [12–19]. The observed phenomena have been immediately interpreted as relaxation processes in the crystalline phase [20]; however, for a long period of time, many experimental facts still remained vague. Several hypotheses describing the molecular mechanism of this phenomenon have been advanced.

Mechanical experiments with PE samples were interpreted according to the general hypothesis concerning the friction between crystallites [21] or between blocks in the crystallites [12, 22]. Furthermore, the model of chain diffusion between crystalline and amorphous phases has been advanced. Chain diffusion is assumed to be provided by the transfer of point-like structural chain defects in the crystallites; these chain defects originate in the amorphous phase and involve conformational (including gauche conformations) twist–compression defects and smooth soliton-like twist–tension defects [24, 25]. When the above defects are transferred along polymer chain and cross the entire crystallite, the polymer chain appears to be shifted by the lattice half period and reoriented by a rotation angle of 180°.

In [26], the abundant experimental data and results on molecular-dynamic simulations have been analyzed, and this analysis demonstrated that the molecular mechanism of chain diffusion in conventional semicrystalline PE samples prepared by melt extrusion can be presented in the following way. A mobile amorphous phase gives rise to nucleation of a smooth twist–tension defect in a crystallite near its boundary; on moving along polymer chain, this defect shifts this chain by one unit (reorientation with a rotation angle of 180°). This nucleation takes place on a tie chain, whose fragments belong to both amorphous and crystalline phases. A chain fragment located in the amorphous phase participates in long-range thermal motions, which involve many (more than ten) CH_2 groups. These motions give rise to force F, which acts on the chain fragment located in the crystalline phase and tends to pull it out from the crystallite. This force acts with a fluctuating intensity; furthermore, a random torque arises. Therefore, occa-

[1] This work was supported by the Russian Foundation for Basic Research, project nos. 04-03-32119 and 05-03-32241.

sional force fluctuations (a strong jerk with twisting) δF trigger the nucleation of the twist–tension defects in the crystallites. The activation energy of chain diffusion approaches the energy of defect nucleation and is equal to ~100 kJ/mol. Let us mention that the nucleation of this defect in the crystallite can be provided only by highly cooperative motions of CH_2 groups in the amorphous chain fragment. Indeed, even at 90°C, the mean kinetic energy of one CH_2 group is only ~4 kJ/mol, whereas 100 kJ/mol should be supplied to the crystallite. This observation explains an extremely low frequency of this process: at 90°C, this value is $\sim 3 \times 10^3$ Hz for the samples prepared by slow cooling from melt.

Molecular-dynamic simulations show [26] that the diffusion coefficient of pointlike chain defects is so high that, in the conventional semicrystalline PE, the observed statistics of flips of C=O dipoles in crystallites coincides with the statistics of nucleation of twist–tension defects bypassing through the crystallites. With consideration for the fact that the profile of the dielectric loss curve is controlled by the statistics of dipolar flips, the experiments directly show the specific features of long-range thermal motions in the amorphous phase.

Some unusual features of dielectric losses in the temperature interval of α_c relaxation in the semicrystalline PE have been observed long ago [20, 27]. First, the loss peak is very narrow, and its half-width at half-height is not higher than decade; second, in the $\varepsilon''/\varepsilon''_{max}$ –f/f_{max} coordinates (ε''_{max} and f_{max} stand for the height and frequency at the maximum of the relaxation process), dielectric losses virtually fit one curve at all temperatures ranging from 50 to 130°C and at pressures varying from 0.02 to 4.25 kbar and for the samples with different thermal prehistories [7].

Only one attempt has been made to explain theoretically the profile of the dielectric loss curve, and this explanation has been performed within the framework of the model of chain diffusion of defects in the sample as in a single chain [28, 29]. According to the above model, the statistics of this process is completely controlled by the specific features of the non-Einstein diffusion of defects. This model involves two parameters: the coefficient of diffusion and the density of defects. However, as was found, the profile of the dielectric loss curve can fit the experimental curve only at physically unreal values of the above parameters: only at very high diffusion coefficient of defects and at very low density of defects. This model cannot be refined by any corrections [30–32].

In our opinion, the dielectric loss curve profile is controlled by the statistics of the development of high fluctuations of force δF induced by chain fragments in the amorphous layer that participate in long-range thermal motions [26]. It can be easily demonstrated (see Appendix) that, when the number of nucleated defects approaching the opposite side of the crystallite is described by the Poisson distribution, the dielectric loss curve should follow the Debye pattern. Since intensive force fluctuations δF are scarce and can be considered independent events, one can expect the Debye character of the dielectric loss curve. However, according to [7, 8, 10], the actual profile of curves is seen to be appreciably different from the Debye curve and, seemingly, is independent of temperature.

From the viewpoint of the molecular model of the process proposed in [26], it seems quite unexpected that the degree of correlation of events δF and, as a consequence, the profile of the dielectric loss curve are independent of temperature. However, in the previous papers on this subject, the accuracy of experimental measurements was rather low, and no measurements at low frequencies were conducted. Furthermore, the authors did not construct the normalized dielectric loss curve

$$\chi''(f) = \frac{\varepsilon''(f)}{\varepsilon'_0 - \varepsilon'_\infty} \quad (1)$$

(where $\varepsilon''(f)$ is the imaginary part of the complex dielectric permittivity at frequency f and ε'_0 and ε'_∞ are the real left-hand and right-hand parts), which allows one to draw certain conclusions concerning the statistics of dipolar flips in crystallite chains (see Section *Normalized Dielectric Loss Curves*).

In this study, we examine the profile of the normalized dielectric loss curve is affected by temperature ranging from 0°C and higher and the thermal prehistory of the sample. Our measurements aim at the experimental verification of the molecular model of chain diffusion between amorphous and crystalline phases in PE proposed in [26]. If this model is correct, the profile of the normalized dielectric loss curve should depend on temperature. In this connection, we will analyze the experimental data obtained in some other studies for the samples with different thermal prehistories [8] and the role of the applied pressure.

EXPERIMENTAL

In this study, we used HDPE samples (brand mark 277-73, GOST [State Standard] 16338-85, OAO KazanOrgSintez) with $M \sim 5 \times 10^5$. Polymer macromolecules contain minor amounts of short side chains, and a distance between them is ~500 of carbon backbone atoms. This type of HDPE seems to be convenient for our studies as it contains a thermostabilizing agent but does not contain any light and UF stabilizers [33].

PE samples were oxidized by UV irradiation. In this case, the samples were prepared as slabs with dimensions of 140 × 120 mm and a thickness of 0.5 mm. The slabs were heated to 160°C. The as-prepared melt was exposed to the UV irradiation for 240 min by using a universal ORKU mercury quartz irradiator; the effective spectral region was 230–400 nm. A distance

between the irradiator and the slab was 180 mm. After cooling, the slab was milled and pressed in a mold with sizes of 140 × 120 × 0.1 mm. The mold was heated for 10 min without any applied external pressure; then, the sample was molded for 10 min at a temperature of 140°C and at a pressure of 50 bar. At the final stage of treatment, four different temperature regimes were used.

Regime 1. Slow cooling down to room temperature at a rate of 1 K/min and at a pressure of 50 bar.

Regime 2. Quenching in an ice water-containing vessel.

Regime 3. Quenching and subsequent annealing for 4 h with an increase in temperature from 90 to 120°C.

Regime 4. Slow cooling with a pause at 105°C, quenching, and annealing at 104°C [22].

The prepared sheet was cut into specimens as disks with a diameter of 40 mm and a thickness of 0.1 mm.

To remove moisture from the sample and from the surface of the body electrodes (gold-decorated disks with a diameter of 32 mm and a thickness of 2 mm), prior to measurements, both samples and electrodes were allowed to stay in a desiccator over silica gel for one week. The necessity of the above measures is related to the fact that the measured dielectric losses are the sum of contributions from dc conductivity and relaxation processes [34]:

$$\varepsilon'' = \varepsilon''_{\text{rel}} + \frac{\sigma_{dc}}{2\pi f \varepsilon_0}.$$

Here, $\varepsilon''_{\text{rel}}$ is a part of dielectric losses provided by the α_c-relaxation process and ε_0 is the universal dielectric constant. At temperatures below 50–70°C, the α_c-relaxation peak in PE is shielded by parasite dielectric losses, and their contribution increases with the decreasing frequency. This effect is related to the electric dc conductivity σ_{dc}, which is primarily controlled by moisture in the sample. The above measures for removal of the residual moisture made it possible to suppress the parasite dielectric losses for ~4 h at frequencies ranging from 10^{-2} and higher. Even at low temperatures, the measurement time of the α_c-relaxation peak was less than 1 h.

For PE samples, the frequency dependences of dielectric permittivity ε' and dielectric losses ε'' were measured at frequencies ranging from 10^{-2} to 10^6 Hz on a Novocontrol BDS-40 broad-band dielectric spectrometer equipped with an active sample cell (Alpha Active Sample Cell) for highly precision dielectric measurements. The relative impedance and the phase angle were estimated with an accuracy of 0.01–0.03% or 0.002°–0.01°, respectively. The measurements were performed at temperatures ranging from 0 to 80°C.

RESULTS AND DISCUSSION

For the PE samples with different thermal prehistories, the temperature dependences of dielectric permittivity and dielectric losses were recorded. Figure 1 shows the experimental spectra of dielectric losses in the temperature interval of the α_c-relaxation process for the samples prepared according to temperature regimes 1, 2, and 3.

Let us mention two features of our results.

First, the removal of moisture from the samples and from the surface of the electrodes allowed marked reduction in the contribution from parasite dielectric losses provided by electric dc conductivity. As a result, the frequency interval of measurements appeared to be widened, and this enabled us for the first time to obtain the frequency dependences of dielectric losses at temperatures down to 0°C.

Second, as follows from Fig. 1, dielectric losses at frequencies above $f_{\max}$ do not decrease to zero with an increase in frequency. Seemingly, this behavior is related to the closely located β-process in the amorphous phase. The length of the high-frequency plateau ε''_∞ does not characterize the α_c-relaxation process but depends on the structure of the amorphous phase in the sample.

Normalized Dielectric Loss Curves

Dielectric losses $\varepsilon''(f)$ in the sample are known to be controlled by many factors. For example, this parameter increases with the amount of active polar dipoles C=O per unit volume of the sample or, in other words, with an increase in the degree of oxidation. Since the α_c-relaxation process involves only those dipoles that exist in the crystallites, at the same degree of oxidation and temperature, the height of the dielectric loss peak increases with an increase in the degree of crystallinity of the sample (cf. Figs. 1a and 1b). Moreover. the height of this peak increases under the action of the applied pressure [10]. Therefore, the experimental dependence $\varepsilon''(f)$ cannot be directly used for the analysis of the physical nature of the α_c-relaxation process.

This analysis requires the use of normalized curves $\chi''(f)$ [see Eq. (1)]. These curves characterize only the statistics of dipole flips. Indeed, according to the linear response theory (e.g. [35]), the Kubo equations [36] for the complex dielectric permittivity $\varepsilon^*(f) = \varepsilon'(f) - i\varepsilon''(f)$ within the approximation of independent dipoles (this approximation is valid for the weakly oxidized PE) lead to the following relationships [37]:

$$\chi'(f) - i\chi''(f) = \frac{\varepsilon^*(f) - \varepsilon'_\infty}{\varepsilon'_0 - \varepsilon'_\infty}$$

$$= -\int_0^\infty dt \exp(-i2\pi ft)\frac{\partial}{\partial t}\bar{C}(t),$$

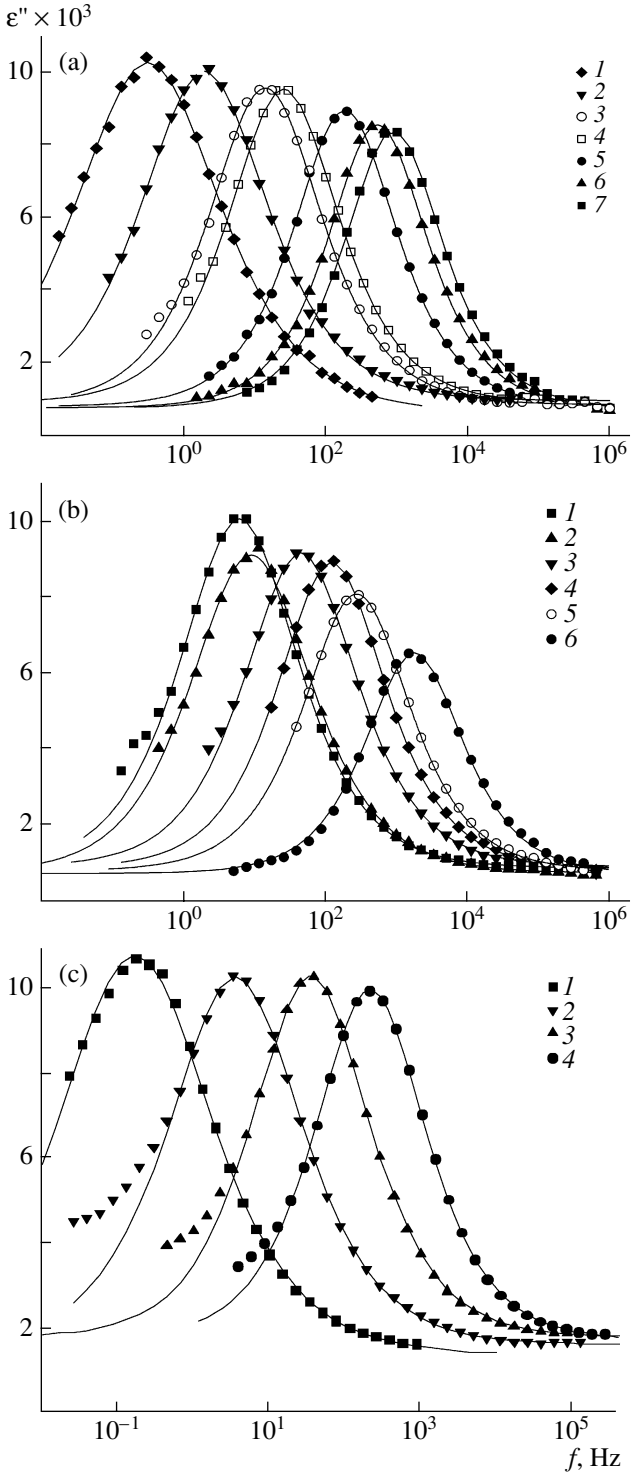

Fig. 1. Frequency dependences ε'' at different temperatures for the samples prepared under regimes (a) 1, (b) 2, and (c) 4. Points refer to the experimental frequency dependence of dielectric losses, and lines refer to the approximation of experimental data by Eq. (2). (a): T = (*1*) 0, (*2*) 18, (*3*) 35, (*4*) 46, (*5*) 60, (*6*) 69, and (*7*) 76°C; (b): T = (*1*) 16, (*2*) 19, (*3*) 35, (*4*) 44, (*5*) 53, and (*6*) 70°C; and (c): T = (*1*) 0, (*2*) 22, (*3*) 43, and (*4*) 56°C.

where $\bar{C}(t) = \dfrac{\langle \boldsymbol{\mu}(0)\boldsymbol{\mu}(t)\rangle}{\langle \boldsymbol{\mu}(0)\boldsymbol{\mu}(0)\rangle}$ and $\boldsymbol{\mu}(t)$ is the dipole moment of a C=O bond; angular brackets denote averaging over the ensemble. For example, if this statistics is described by the Poisson law (the sequence of independent events), we deal with the Debye curve (see Appendix); the Bose–Einstein statistics leads to a less intensive and broader curve.

For the further analysis of dipole flips, all experimental frequency dependences ε''(f) were plotted as normalized curves χ''(f); to this end, the following original procedure of their construction was proposed.

First of all, the experimental value $\varepsilon_0' - \varepsilon_\infty'$ is a difference between large numbers; hence, its direct use leads to serious errors. However, as follows from the experimental frequency dependences of ε'' (Fig. 1), the α_c-relaxation process is symmetric and can be described as the Debye process. Relaxation processes of this kind can be approximated by the Cole–Cole dependence [34]. Within this approximation, the complex dielectric permittivity is described by curve $\varepsilon^*(f) = \varepsilon_\infty' + \dfrac{\varepsilon_0' - \varepsilon_\infty'}{1 + \left(i\dfrac{f}{f_{\max}}\right)^{1-\alpha}}$, where i is the imaginary unit, and parameter α describes a deviation from the Debye character. This approximation allows estimation of the difference $\varepsilon_0' - \varepsilon_\infty'$ with a higher accuracy as compared with the estimation directly from the experimental frequency dependence ε'(f).

Furthermore, to gain accurate approximation of the dielectric loss curve, the imaginary part of the Cole–Cole equation should also involve the plateau value ε_∞'', which corresponds to saturation of the dielectric loss curve at high frequencies. Therefore, the equation for approximation of the complex part of dielectric permittivity takes the following form:

$$\varepsilon''(f) = \frac{(\varepsilon_0' - \varepsilon_\infty')\left(\dfrac{f}{f_{\max}}\right)^{1-\alpha}\cos\dfrac{\alpha\pi}{2}}{1 + 2\left(\dfrac{f}{f_{\max}}\right)^{1-\alpha}\sin\dfrac{\alpha\pi}{2} + \left(\dfrac{f}{f_{\max}}\right)^{2(1-\alpha)}} + \varepsilon_\infty'' \quad (2)$$

This approximation makes it possible to estimate the plateau region height ε_∞'', the frequency $f_{\max}$ corresponding to the maximum dielectric losses, parameter α characterizing the deviation from the Debye curve, and a difference in dielectric permittivities $\varepsilon_0' - \varepsilon_\infty'$ in the region of the relaxation process.

As follows from Fig. 1, the experimental data are well described by Eq. (2). Parameters of Eq. (2) corresponding to the experimental data shown in Fig. 1 are listed in the table.

The Dependence of Frequency f_{max} on Temperature and Thermal Prehistory of the Sample

Figure 2 displays the temperature dependence of frequency f_{max} for different samples. As expected, in the case of the quenched sample, the straight line $\log f_{max}(1/T)$ is higher than those of the samples prepared under regimes 1, 3, and 4 because its degree of crystallinity is lower. In the quenched sample, its amorphous phase is more mobile, and the frequency of defect nucleation induced by the amorphous regions of tie chains should be higher. As anticipated, the annealing of the quenched sample (at any of the selected temperatures) and subsequent slow cooling lead to the state in the sample that is equivalent to slow cooling. The complicated preparation regime 4 entails the same results: f_{max} coincides with the corresponding frequency of the slowly cooled sample.

Dependence of the Profile of the Normalized Dielectric Loss Curve on Temperature and Thermal Prehistory of the Sample

Figure 3 shows the normalized dielectric loss curves plotted against the normalized frequency (f/f_{max} is plotted along the abscissa axis) $\chi''(f/f_{max}) = \frac{\varepsilon''(f/f_{max}) - \varepsilon''_\infty}{\varepsilon'_0 - \varepsilon'_\infty}$ [parameters ε''_∞, $\varepsilon'_0 - \varepsilon'_\infty$, and f_{max} are estimated from approximation of the experimental dependence $\varepsilon''(f)$ by Eq. (2)] for the sample prepared under regime 1. As follows from Fig. 2, the profile of the normalized dielectric loss curve strongly depends on temperature. With the increasing temperature, the loss peak becomes broader, and this curve approaches the Debye curve. For all other samples, the behavior of the corresponding normalized curves appears to be quite similar.

To describe deviation of the normalized curve from the Debye profile, it seems convenient to use, instead of parameter α, $\tan\left(\frac{\pi}{4}(1-\alpha)\right)$ that is equal to the peak height χ''_{max} in the normalized dielectric loss curve. Figure 4 illustrates the temperature dependence of this parameter for different samples. As follows from Figs. 3 and 4, the peak height of the normalized curves increases with temperature. In the temperature interval under study, this parameter linearly depends on the reciprocal temperature:

$$\chi''_{max} = B - \frac{D}{T}$$

For all samples, except the quenched sample, constants D and B are the same; for the quenched sample, straight line $\chi''_{max}(1/T)$ appears to be much higher than the corresponding curves for all other samples.

Parameters of approximation curves [Eq. (2)] for dielectric losses of the samples prepared under regimes 1, 2, and 4

T, °C	$(\varepsilon'_0 - \varepsilon'_\infty) \times 10^2$	f_{max}, Hz	α	$\varepsilon''_\infty \times 10^4$
		Regime 1		
0	3.58	0.343	0.400	7.2
18	3.22	1.99	0.347	10
35	2.79	14.3	0.289	89
46	2.76	25.4	0.289	92
60	2.40	188	0.242	8.4
69	2.21	541	0.220	8.0
76	2.16	910	0.214	7.8
		Regime 2		
16	3.05	6.28	0.309	9.0
19	2.86	9.18	0.327	7.7
35	2.76	44.3	0.312	8.3
44	2.48	125	0.269	8.9
53	2.22	279	0.265	8.2
70	1.62	1823	0.209	7.5
		Regime 4		
0	3.76	0.176	0.411	13.8
22	3.01	3.78	0.336	16.3
43	2.65	36.2	0.274	17.9
56	2.46	218	0.247	17.2

Let us compare our curves with the results published by other authors. The dependence of dielectric losses on the thermal prehistory of the samples was studied in [8]. Figure 5 shows that, even though the measurements were performed in a narrower frequency interval, experimental curves can be approximated by the Cole–Cole curve and, hence, the proposed approach can be used for construction of the normalized curves.

Figure 6 shows the normalized dielectric loss curves as a function of normalized frequency plotted from the data reported in [8] and our curves obtained at a close temperature of ~70°C. For the samples with different thermal prehistories, the $\chi''(f/f_{max})$ curves appear to be different at similar temperatures. As compared with the literature data, in the case of our experimental results, this difference is not that dramatic. This trend is also observed for the plots with central frequency (by the same reason). As follows from Fig. 6, at the same temperature, the samples with different thermal prehistories are characterized by different event correlations with respect to the development of intensive force fluctuations δF induced in the amorphous chain fragments. Let us mention that the curve corresponding to the quenched sample with its loosened and mobile amorphous phase is higher (and approaches the Debye curves corresponding to independent fluctuations δF) than the curve corresponding to the slowly cooled sam-

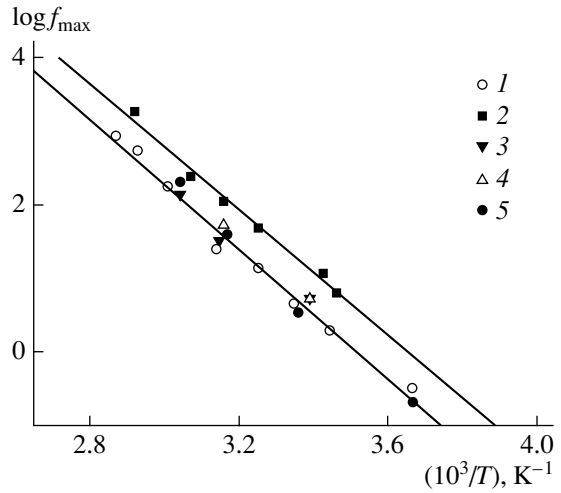

Fig. 2. Temperature dependence of dielectric loss maximum f_{max} for the α_c-relaxation process for the samples with different thermal prehistories prepared under regimes (*1*) 1, (*2*) 2, 3 and annealing at T_{an} = (*3*) 90 and (*4*) 110°C, and (*5*) 4.

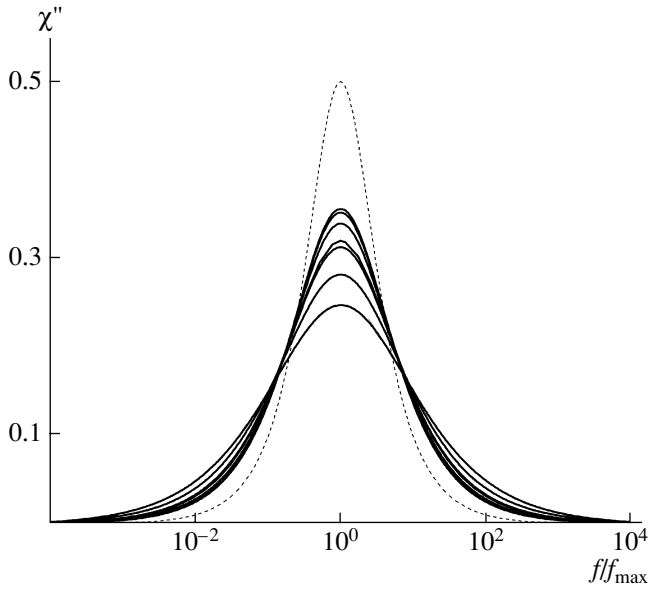

Fig. 3. Normalized dielectric loss curves as a function of normalized frequency for the slowly cooled sample (regime 1). Dielectric loss maximum increases with temperature (76, 69, 60, 46, 35, 18, and 0°C). For comparison, the Debye curve is shown by the dotted line.

ple, in which volume of the amorphous phase is smaller, and its mobility is lower. Therefore, the analysis of the dielectric loss curve profile (the statistics of dipole flips) allows one to conclude that preparation of the sample with the "compressed" amorphous phase is equivalent to cooling of the sample with a loosened amorphous phase.

Pressure Dependence of the Normalized Dielectric Loss Curve

The dependence of dielectric losses on the applied pressure was studied in [10]. Even though the number of the experimental points is low, they can be approximated by Eq. (2) with a fair accuracy. Figure 7 shows the approximated curves, and the corresponding normalized dielectric loss curves plotted against the normalized frequency are shown in Fig. 8. As is seen, the effect of the applied pressure on the relaxation process is similar to that of cooling (Fig. 8). The observed behavior (the reduced frequency of dipole flips and the broadened peak of the normalized dielectric loss curve under the applied pressure) can be explained in terms of the proposed hypothesis concerning the molecular mechanism of this process [26]. Indeed, under the applied pressure, long-range thermal motions in the amorphous phase leading to the pull-out of polymer chains from the crystallites and concomitant dipole flip are retarded and become more correlated. A similar tendency is observed with the decreasing temperature.

As follows from Figs. 5–8, the effect of the thermal prehistory of the sample and the applied pressure on the profile of the normalized dielectric loss curve can be observed even for the data reported in the early publications even though the number of the experimental points at high and low frequencies is small.

CONCLUSIONS

The analysis of chain diffusion between crystalline and amorphous phases in PE [26] allows one to expect that the high-temperature α_c relaxation in PE crystal-

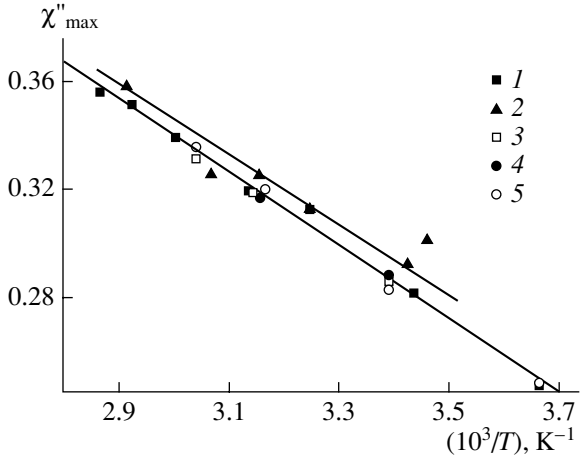

Fig. 4. Maxima of the normalized dielectric loss curves vs. reciprocal temperature for the samples prepared under regimes (*1*) 1, (*2*) 2, 3 and annealing at T_{an} = (*3*) 90 and (*4*) 110°C, and (*5*) 4.

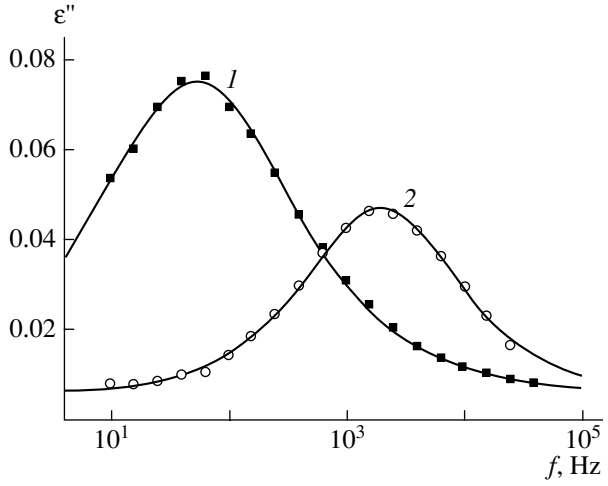

Fig. 5. Dielectric loss curves at close temperatures for samples (*1*) A94–1CE and (*2*) A94-1Q [(*1*) sample crystallized at a pressure of 5.3 kbar at 221°C and slowly cooled under pressure and (2) quenched sample]. Points refer to the experimental data from [8], and curves refer to approximation of the experimental data according to Eq. (2).

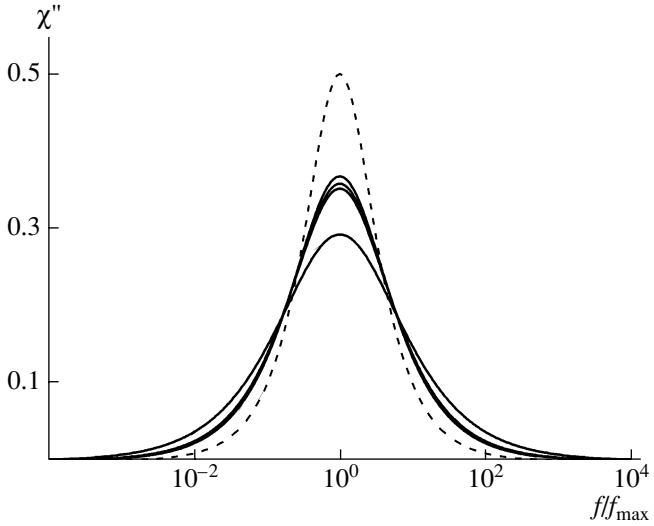

Fig. 6. Normalized dielectric loss curves as a function of normalized frequency for the experimental data reported in [8] and presented in Fig. 5 and for our experimental data obtained at close temperatures (68–70°C). The curves correspond to the following samples (in the order of decreasing dielectric loss maximum): A94–1Q (the quenched sample) [8]; the sample prepared under regime 2; the sample prepared under regime 1; and A94–1CE (crystallized at a pressure of 5.3 kbar at 221°C; slowly cooled under pressure) [8]. For comparison, the Debye curve is shown by the dotted line.

lites (the α_c peak) should be described by the temperature-dependent profiles of the normalized dielectric loss curves. In this study, this tendency has been found.

With an increase in temperature, the loss peak becomes higher and narrower; its profile approaches the Debye curve, which corresponds to the Poisson statistics of dipole flips (sequence of independent events). In the temperature interval under study, the effect of temperature T (in Kelvin) on the height of the normalized dielectric loss curve is described by the following equation $\chi''_{max} = B - \frac{D}{T}$, where constant D is the same for all PE samples; for the quenched sample, constant B appears to be somewhat higher than that of the slowly cooled sample. In the temperature interval under study (0–80°C), as compared with the Debye curves, all dielectric loss curves are seen to be wider and lower. This fact indicates bunching of dipole flip events. The application of pressure to the sample s is equivalent to its cooling and a decrease in the fraction of the amorphous phase.

In our opinion, this evidence provides a reliable experimental validation of the molecular model for the α_c-relaxation process proposed in [26].

APPENDIX

Autocorrelation dipole function $C(t)$ reflects the random process with parameter t, which presents the sum of random processes $C(t) = 1 + \sum_{i=0}^{N_t} B_i(t, t_i)$, where N_t is the number of defects that approach a dipole at time t, and $B_i(t, t_i)$ describes changes in $C(t)$ after ith flip at time t_i. The distribution function $C(t)$ is defined as $R(v, t) = P\{C(t) \le v\} = \int_{-\infty}^{v} dy r(y, t)$, where $r(y, t)$ is the density function of $C(t)$. The first-order derivative

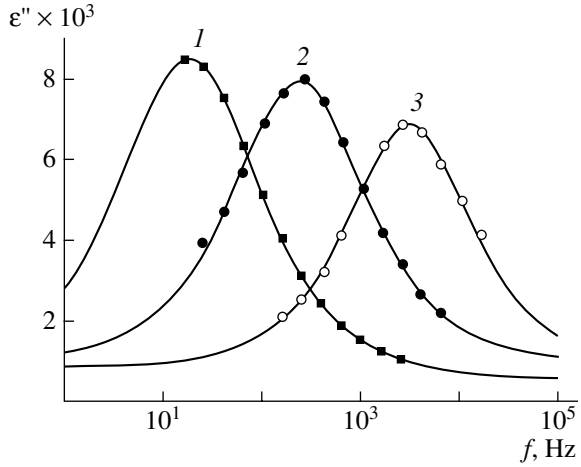

Fig. 7. Dielectric loss curves for the PE sample at different pressures: (*1*) 4.25, (*2*) 1.77, and (*3*) 0.02 kbar [10]. Points refer to the experimental data, and approximation curves were obtained from Eq. (2).

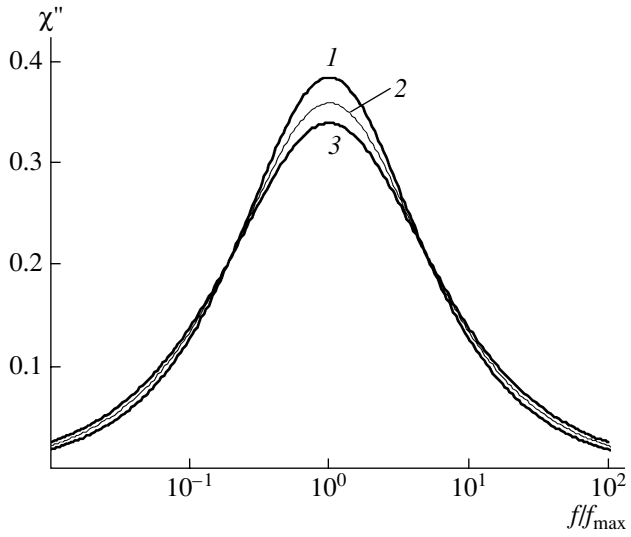

Fig. 8. Normalized dielectric loss curves plotted against the normalized frequency for the experimental data [10] shown in Fig. 7. Curves (in the order of decreasing dielectric loss maximum) correspond to a pressure of (*1*) 0.02, (*2*) 1.77, and (*3*) 4.25 kbar.

of the characteristic function with this density $\phi_t(w) = \int_{-\infty}^{\infty} dy \exp(iwy)\, r(y, t)$ with respect to w is proportional to the ensemble average with respect to $C(t)$: $\bar{C}(t) = -i\frac{\partial}{\partial w}\phi_t(w)|_{w=0}$. Since

$$R(v, t) = \sum_{n=0}^{\infty} P\{C(t) \le v | N_t = n\} P\{N_t = n\},$$

$$\phi_t(w) = \sum_{n=0}^{\infty} P\{N_t = n\} \times \int_{-\infty}^{\infty} dy \exp(iwy) \frac{d}{dy} P\{C(t) \le y | N_t = n\}$$

Here, integral is the characteristic function representing the sum of independent random variables and, hence, the product of their characteristic functions. Assuming that the dipole flip $B_i(t, t_i)$ is described by the simplest relationship (the instant flip at time t_i)

$$B^{-}(t - t_i) = \begin{cases} 0, & t - t_i < 0 \\ -2, & t - t_i \ge 0 \end{cases} \text{ at odd } i,$$

$$B^{+}(t - t_i) = \begin{cases} 0, & t - t_i < 0 \\ 2, & t - t_i \ge 0 \end{cases} \text{ at even } i,$$

we arrive at

$$\bar{C}(t) = \sum_{n=0}^{\infty} (-1)^n P\{N_t = n\}$$

This sum can be readily calculated for the Poisson process (the independent sequence of events) as

$$\bar{C}^{(P)}(t) = \sum_{n=0}^{\infty} (-1)^n P^{(P)}\{N_t = n\}$$

$$= \sum_{n=0}^{\infty} (-1)^n \frac{(t/\tau_0)^n}{n!} \exp(-t/\tau_0) = \exp(-2t/\tau_0)$$

After the Fourier transform, we find that, for the Poisson process, the normalized dielectric loss curve is described by the Debye curve:

$$\chi''_{(P)}\left(\frac{f}{f_{max}}\right) = \frac{(f/f_{max})}{1 + (f/f_{max})^2}$$

ACKNOWLEDGMENTS

We would like to express our sincere gratitude to E.F. Oleinik for the Novocontrol BDS-40 dielectric spectrometer and Alpha Active Sample Cell and fruitful discussions.

REFERENCES

1. K. Schmidt-Rohr and H. W. Spiess, Macromolecules **24**, 5288 (1991).
2. W.-G. Hu, C. Boeffel, and K. Schmidt-Rohr, Macromolecules **32**, 1611 (1999).
3. G. P. Mikhailov, A. N. Lobanov, and B. I. Sazhin, Zh. Tekh. Fiz. **24**, 1553 (1954).
4. G. P. Mikhailov, S. P. Kabin, and B. I. Sazhin, Zh. Tekh. Fiz. **25**, 590 (1955).
5. G. P. Mikhailov, S. P. Kabin, and T. A. Krylova, Zh. Tekh. Fiz. **27**, 2050 (1957).
6. K. Schmieder and K. Wolf, Kolloid Z. Z. Polym. **134**, 157 (1953).
7. Y. Ishida and K. Yamafuji, Kolloid Z. Z. Polym., B **202**, 26 (1965).
8. C. R. Ashcraft and R. H. Boyd, J. Polym. Sci., Part B: Polym. Phys. **14**, 2153 (1976).
9. R. H. Boyd and T. Yemni, Polym. Eng. Sci. **14**, 1023 (1979).
10. J. A. Sayre, St. R. Swanson, and R. H. Boyd, J. Polym. Sci., Part B: Polym. Phys. **16**, 1739 (1978).
11. M. S. Graff and R. H. Boyd, Polymer **35**, 1797 (1994).
12. M. Takayanagi, in *Molecular Basis of Transition and Relaxation*, Ed. by D. J. Meier (Midland Macromolecular Monographs Gordon and Breach, London, 1978), Vol. 4, p. 117.

13. N. G. McCrum, in *Molecular Basis of Transition and Relaxation*, Ed. by D. J. Meier (Midland Macromolecular Monographs Gordon and Breach, London, 1978), Vol. 4, p. 167.
14. M. Matsuo, C. Sawatari, and T. Ohhata, Macromolecules **21**, 1317 (1988).
15. M. Matsuo, Y. Bin, Ch. Xu, et al., Polymer **44**, 4325 (2003).
16. H. Zhou and G. L. Wilkes, Macromolecules **30**, 2412 (1997).
17. J. F. Mano, R. A. Sousa, R. L. Reis, et al., Polymer **42**, 6187 (2001).
18. Y. Men, J. Rieger, H.-F. Endeler, and D. Lilge, Macromolecules **36**, 4689 (2003).
19. I. Kolesov, R. Androsch, and H.-J. Radusch, Macromolecules **38**, 445 (2005).
20. R. H. Boyd, Polymer **26**, 323 (1985).
21. N. Saito, K. Okano, S. Iwayanagi, and T. Hideshima, in *Solid State Physics*, Ed. by F. Seitz and D. Turnbull (Academic, New York, 1963), Vol. 14, p. 453.
22. H. Kawai, S. Suehiro, T. Kyu, and A. Shimomura, Polym. Eng. Rev. **3**, 109 (1983).
23. D. H. Reneker, B. M. Fanconi, and J. J. Mazur, Appl. Phys. **48**, 4032 (1977).
24. M. S. Mansfield and R. H. Boyd, J. Polym. Sci., Part B: Polym. Phys. **16**, 1227 (1978).
25. M. S. Mansfield, Chem. Phys. Lett. **69**, 383 (1980).
26. E. A. Zubova, N. K. Balabaev, and L. I. Manevitch, Polymer **48**, 1802 (2007).
27. R. H. Boyd, Polymer **26**, 1123 (1985).
28. J. L. Skinner and P. G. Wolynes, J. Chem. Phys. **73**, 4015, 4022 (1980).
29. J. L. Skinner and Y. H. Park, Macromolecules **17**, 1735 (1984).
30. K. J. Wahlstrand, J. Chem. Phys. **82**, 5247 (1985).
31. K. J. Wahlstrand and P. G. Wolynes, J. Chem. Phys. **82**, 5259 (1985).
32. K. J. Wahlstrand, Polymer **29**, 256, 263 (1988).
33. V. G. Makarov and V. B. Koptenarmusov, *Commercial Thermoplasics: A Handbook* (Khimiya, Moscow, 2003) [in Russian].
34. T. L. Chelidze, A. I. Derevyanko, and O. D. Kurilenko, *Electric Spectroscopy of Heterogeneous Systems* (Naukova Dumka, Kiev, 1977) [in Russian].
35. D. N. Zubarev, *Nonequilibrium Statistical Thermodynamics* (Nauka, Moscow, 1998) [in Russian].
36. R. Kubo, J. Phys. Soc. Jpn. **12**, 570 (1957).
37. G. Williams and D. C. Watts, Trans. Faraday Soc. **66**, 80 (1970).

SPELL: 1. KazanOrgSintez